Interferometer phase noise due to beam misalignment on diffraction gratings

Deepali Lodhia,[1,*] Daniel Brown,[1] Frank Brückner,[1] Ludovico Carbone,[1] Paul Fulda,[2] Keiko Kokeyama,[3] and Andreas Freise[1]

[1]*School of Physics and Astronomy, University of Birmingham, Birmingham, B15 2TT, UK*
[2]*Department of Physics, University of Florida, Gainesville, Florida, 32611-8440, USA*
[3]*Department of Physics and Astronomy, Louisiana State University, Baton Rouge, Louisiana, 70803-4001, USA*

[*]*dl@star.sr.bham.ac.uk*

Abstract: All-reflective interferometer configurations have been proposed for the next generation of gravitational wave detectors, with diffractive elements replacing transmissive optics. However, an additional phase noise creates more stringent conditions for alignment stability. A framework for alignment stability with the use of diffractive elements was required using a Gaussian model. We successfully create such a framework involving modal decomposition to replicate small displacements of the beam (or grating) and show that the modal model does not contain the phase changes seen in an otherwise geometric planewave approach. The modal decomposition description is justified by verifying experimentally that the phase of a diffracted Gaussian beam is independent of the beam shape, achieved by comparing the phase change between a zero-order and first-order mode beam. To interpret our findings we employ a rigorous time-domain simulation to demonstrate that the phase changes resulting from a modal decomposition are correct, provided that the coordinate system which measures the phase is moved simultaneously with the effective beam displacement. This indeed corresponds to the phase change observed in the geometric planewave model. The change in the coordinate system does not instinctively occur within the analytical framework, and therefore requires either a manual change in the coordinate system or an addition of the geometric planewave phase factor.

OCIS codes: (050.1950) Diffraction gratings(050.1960); Diffraction theory; (050.5080) Phase shift.

References and links

1. G. Harry, "Advanced Ligo: the next generation of gravitational wave detectors," Class. Quantum Grav. **27**, 084006 (2010).
2. T. Accadia, F. Acernese, F. Antonucci, P. Astone, G. Ballardin, F. Barone, M. Barsuglia, A. Basti, T. Bauer, M. Bebronne et al., "Status of the Virgo project," Class. Quantum Grav. **28**, 114002 (2011).
3. B. Willke, P. Ajith, B. Allen, P. Aufmuth, C. Aulbert, S. Babak, R. Balasubramanian, B. Barr, S. Berukoff, A. Bunkowski et al., "The GEO-HF project," Class. Quantum Grav. **23**, S207 (2006).
4. R. Drever, "Concepts for extending the ultimate sensitivity of interferometric gravitational wave detectors using non-transmissive optics with diffractive or holographic coupling," in *Proceedings of the Seventh Marcel Grossman Meeting on General Relativity*, M. Keiser and R. T. Jantzen, eds. (World Scientific, 1995).
5. A. Bunkowski, O. Burmeister, T. Clausnitzer, E. Kley, A. Tünnermann, K. Danzmann, and R. Schnabel, "Diffractive optics for gravitational wave detectors," J. Phys.: Conf. Ser. **32**, 333–338 (2006).

#187849 - $15.00 USD Received 27 Mar 2013; revised 11 Oct 2013; accepted 16 Oct 2013; published 22 Nov 2013

6. A. Bunkowski, O. Burmeister, P. Beyersdorf, K. Danzmann, R. Schnabel, T. Clausnitzer, E. Kley, and A. Tünnermann, "Low-loss grating for coupling to a high-finesse cavity," Opt. Lett. **29**, 2342–2344 (2004).
7. M. Britzger, D. Friedrich, S. Kroker, F. Brückner, O. Burmeister, E. Kley, A. Tünnermann, K. Danzmann, and R. Schnabel, "Pound-Drever-Hall error signals for the length control of three-port grating coupled cavities," Appl. Opt. **50**, 4340–4346 (2011).
8. D. Friedrich, O. Burmeister, A. Bunkowski, T. Clausnitzer, S. Fahr, E. Kley, A. Tünnermann, K. Danzmann, and R. Schnabel, "Diffractive beam splitter characterization via a power-recycled interferometer," Opt. Lett. **33**, 101–103 (2008).
9. S. Kroker, T. Käsebier, F. Brückner, F. Fuchs, E. Kley, and A. Tünnermann, "Reflective cavity couplers based on resonant waveguide gratings," Opt. Express **19**, 16466–16479 (2011).
10. S. Wise, V. Quetschke, A. Deshpande, G. Mueller, D. Reitze, D. Tanner, B. Whiting, Y. Chen, A. Tünnermann, E. Kley et al., "Phase effects in the diffraction of light: beyond the grating equation," Phys. Rev. Lett. **95**, 13901 (2005).
11. A. Freise, A. Bunkowski, and R. Schnabel, "Phase and alignment noise in grating interferometers," New J. Phys. **9**, 433 (2007).
12. J. Hallam, S. Chelkowski, A. Freise, S. Hild, B. Barr, K. Strain, O. Burmeister, and R. Schnabel, "Coupling of lateral grating displacement to the output ports of a diffractive Fabry-Perot cavity," J. Opt. A, **11**, 085502 (2009).
13. A. Freise, G. Heinzel, H. Lück, R. Schilling, B. Willke, and K. Danzmann, "Frequency-domain interferometer simulation with higher-order spatial modes," Class. Quantum Grav. **21**, S1067 (2004).
14. D. Lodhia, F. Brückner, L. Carbone, P. Fulda, K. Kokeyama, and A. Freise, "Phase effects in Gaussian beams on diffraction gratings," J. Phys.: Conf. Ser. **363** 012014 (2012).
15. R. Drever, J. Hall, F. Kowalski, J. Hough, G. Ford, A. Munley, and H. Ward, "Laser phase and frequency stabilization using an optical resonator," Appl. Phys. B, **31**, 97–105 (1983).
16. A. Taflove and S. C. Hagness, *Computational Electrodynamics: The Finite-Difference Time-Domain Method* (3rd ed., Artech House, 2005).
17. K. Yee, "Numerical solution of initial boundary value problems involving Maxwell's equations in isotropic media," IEEE Trans. Antennas Propag. **14**, 302–307 (1966).
18. D. Brown, D. Friedrich, Frank Brückner, L. Carbone, R. Schnabel and A. Freise, "Invariance of waveguide grating mirrors to lateral displacement phase shifts," Opt. Letters, 38, 1844–1846 (2013).

1. Introduction

A network of ground-based laser interferometric observatories, including Advanced LIGO [1], Advanced VIRGO [2] and GEO HF [3], are in the midst of being upgraded to highly sensitive second-generation gravitational wave detectors. Scientists are confident of obtaining the first direct detection of gravitational waves using the modified instruments, based on the experience gained through the first-generation operation. A simultaneous effort is also underway to devise new concepts to increase detector sensitivities even further, in an attempt to introduce a new era of gravitational-wave astronomy.

One promising approach for the next-generation of interferometers is to replace conventional partly-transmissive optics, such as beam splitters and cavity couplers, by reflective dielectric diffraction gratings [4]. An all-reflective interferometer setup has the potential to significantly reduce thermal effects caused by absorption of high-power laser light in the optical substrates. These thermal distortions are known as a significant challenge limiting the light power that can be utilized in current and future interferometer gravitational wave detectors. Additionally, reflective diffractive gratings allow for a broader choice of opaque substrate materials with a potential for superior mechanical properties.

Since the initial concept of all-reflective interferometry, various groups around the world have built on the notion and presented experimental proof of their feasibility and compatibility with standard interferometric techniques. Such work includes replacing conventional cavity input mirrors and characterising 2-port [5] and 3-port cavity couplers [6, 7], as well as a full operation of a 4-port reflectively coupled Michelson interferometer [8]. A very recent proposal also demonstrated reflective coupling without the need of adding a multilayer coating, which would further reduce thermal effects associated with the coating stack itself [9]. However, due to the broken symmetry of light deflection, the use of diffraction gratings introduces an additional

#187849 - $15.00 USD Received 27 Mar 2013; revised 11 Oct 2013; accepted 16 Oct 2013; published 22 Nov 2013

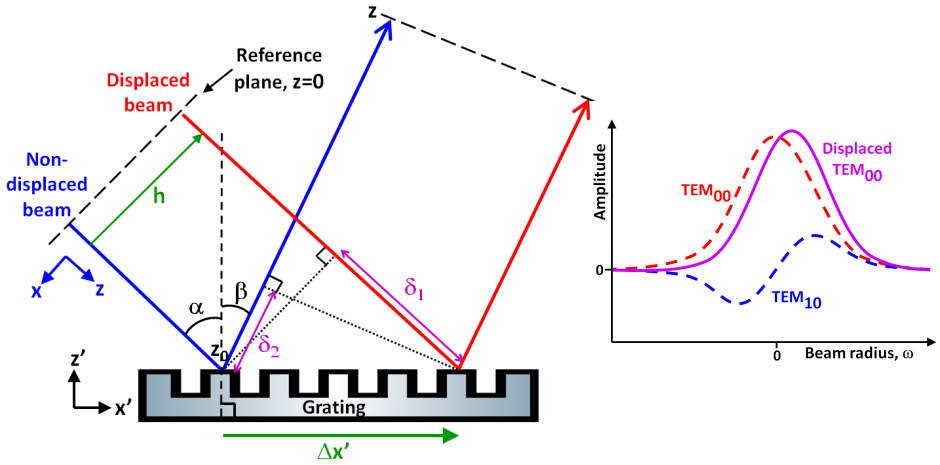

Fig. 1. *Left*: Diffraction of light into the m-th diffraction order when the grating is displaced by amount $\Delta x'$ relative to the beam. A grating displacement $\Delta x'$ corresponds to a parallel beam displacement h, and induces an output optical path length change of ΔP according to Eq. (2). *Right*: A displaced zero-order mode beam can be decomposed into non-displaced zero-order and first-order mode beams for fixed coordinate systems.

coupling from alignment noise to output phase noise [10, 11].

Figure 1 (left) illustrates how the phase noise arises from a simple misalignment of a beam. An incident beam with vacuum wavelength λ is diffracted from a reflective diffraction grating with period d into the m-th diffraction order (we consider only one diffraction order m). The angle conventions imply a positive incidence angle α, while the diffraction angles β_m can be both negative and positive. According to the grating equation

$$\sin\alpha + \sin\beta_m = \frac{m\lambda}{d}, \tag{1}$$

it follows that the diffraction angle β_m of a certain functional output coupling port will be different from the incident angle α (except for the zero-order specular order). It is discernible from a purely geometrical consideration that a slight lateral displacement of either the grating, $\Delta x'$, or the beam, h, induces a shift in the optical path length of $\Delta P = \delta_1 + \delta_2$ (where δ_2 is negative). This shift is related to the displacement $\Delta x'$ via the grating equation (1) [11]:

$$\Delta P = \delta_1 + \delta_2 = -\Delta x' \frac{m\lambda}{d}. \tag{2}$$

In other words, when a grating is displaced by an amount $\Delta x = d$, a diffracted beam will undergo a total phase shift of 2π radians, with a dependency on the diffraction order m. Given this phase noise, the use of gratings imposes more challenging requirements for the suspension and isolation systems for optical components compared to conventional interferometric settings with a natural symmetry of light reflection. Recently, we proposed an advanced readout for the ports of a grating coupler which suppressed phase noise originating from lateral grating displacement. The result was a factor of 20 relaxation in the lateral displacement suspension requirement at 10 Hz [12].

There is an urgent need to assess these requirements in further detail with the use of realistic interferometry simulation tools based on a Gaussian description, such as FINESSE [13]. These Gaussian-based simulation tools are restricted to fixed coordinate systems, and therefore rely

#187849 - $15.00 USD Received 27 Mar 2013; revised 11 Oct 2013; accepted 16 Oct 2013; published 22 Nov 2013

on the technique of decomposing the laser beam into higher-order modes. Yet, effects due to grating-related phase noise were solely investigated using geometric planewave considerations because they allow for a straight-forward computation of the phase shift; these plane-wave models are not a realistic representation of the Gaussian-based simulation tools.

In this paper, we present a fully analytical Gaussian framework to describe a small beam (or grating) displacement by means of a first-order modal decomposition of the beam. This modal model is the standard approach for off-axis beams in Gaussian-based simulation tools, as depicted in Fig. 1 (right). We examine the phase behaviour of the displaced beam and compare the results for the modally decomposed model with those from the geometric planewave approach (preliminary studies and results can be found in [14]). We justify the use of modal decomposition within the Gaussian framework through experimental means: we investigate the phase behaviour in a zero-order and first-order beam imprinted by diffraction from a grating in order to determine whether the phase is dependent on the beam shape. The experimental setup consisted of a table-top Mach-Zehnder interferometer, and a reflective diffraction grating placed in one of the arms. Using a Gaussian description as the core basis, a rigorous time-domain simulation tool was developed to firstly verify the phase dependency on the beam shape, thereby further supporting the experimental findings. Secondly, a direct phase comparison of a diffracted beam was made between an actual beam displacement and a modally decomposed model. We finally corroborate the inclusion of the 'geometric planewave phase factor' for alignment stability computations involving diffractive elements when using Gaussian-based simulation tools.

2. A framework for a Gaussian beam displacement

The aim of this section is to establish an analytical framework derived from a Gaussian description of modal decomposition. Using the phase distribution of a non-displaced beam as a reference, we then distinguish the phase accumulation of a displaced beam using two approaches: an actual geometrical translation of the beam or grating, and modal decomposition by adding a higher-order mode.

To clarify the setup, we refer to Fig. 1 (left), where a non-displaced and displaced beam both propagate from one reference plane (black dashed line) and undergo grating diffraction before reaching a second reference plane. The grating is orientated to lie in the x'-y' plane, with the grooves parallel to the y'-axis. The beam propagates along the z-axis, and we are concerned with changes to the beam parameters only in the x-z direction of the beam. Note that the coordinate system of the beam (x,y,z) is rotated by the angle α relative to the coordinate system of the grating (x',y',z'). The grating displacement $\Delta x'$ is expressed in terms of the beam displacement h and the angle of incidence α using the following relation:

$$h = \Delta x' \cos\alpha. \tag{3}$$

2.1. Beam translation and modal decomposition of a Gaussian beam

We begin by considering the description of a displaced Gaussian beam in terms of both a geometric translation and a modal decomposition (see Appendix A for a thorough description of a Gaussian beam). Without loss of generality, we initially consider the beam at the waist position, z_0, where the waist size is ω_0. We also assume a displacement of the beam along the x-axis, rather than a displacement of the grating along the x'-axis, due to the symmetry of the setup [10]. If we introduce a displacement h to a fundamental beam, the Hermite-Gauss function of the translated beam, $u_0^t(x,z_0)$, is defined at the waist as:

$$u_0^t(x,z_0) = \left(\frac{2}{\pi}\right)^{\frac{1}{4}} \frac{1}{\sqrt{\omega_0}} \exp\left(-\frac{(x-h)^2}{\omega_0^2}\right), \tag{4}$$

#187849 - $15.00 USD Received 27 Mar 2013; revised 11 Oct 2013; accepted 16 Oct 2013; published 22 Nov 2013

where the superscript t indicates a geometric translation along the x-axis. Next, we can substitute Eq. (11) into an expansion of Eq. (4) (see Appendix A). Since typical grating displacements are extremely small compared to the beam waist, we can use the approximation $h/\omega_0 \ll 1$ and apply a first-order Taylor expansion to obtain the expression

$$u_0^d(x,z_0) = u_0(x,z_0) + \frac{h}{\omega_0}u_1(x,z_0), \tag{5}$$

with the superscript d to denote a first-order modal decomposition. Equation (5) validates the theorem that the properties of a slightly displaced zero-order mode beam can be characterised by a decomposition into zero-order and first-order modes (as illustrated in Fig. 1 (right)).

2.2. Phase terms

Having established an expression to describe a displaced beam by means of modal decomposition, the phase of the decomposed beam can be examined more closely. The specific phase terms can be better understood when the beam is propagated away from the waist, and z_0 is replaced by the propagation distance along the optical axis, z. Away from the waist, extra parameters have to be taken into consideration, such as the radius of curvature of the wavefronts, R_C, the Gouy phase, $\Psi(z)$, and the wave number k (defined as $k = 2\pi/\lambda$). Equations (8) and (10) in Appendix A reveal three contributions to the overall phase of a beam: $\exp(-ikz)$, $\exp\left(i\frac{1}{2}\Psi\right)$ and $\exp\left(-i\frac{kx^2}{2R_C}\right)$. Using the general form, $\exp(-i\theta)$, the phase of a beam, θ, at any given point in the x-z plane is specified as

$$\theta_{f,t,d} = kz - \frac{1}{2}\Psi + \phi_{f,t,d}, \tag{6}$$

where the subscripts f, t and d correspond to the fundamental non-translated, translated and modally decomposed beams, respectively. The individual terms for $\phi_{f,t,d}$ are detailed in Appendix B. We now have a Gaussian-based framework to exactly describe the phase of non-displaced and displaced beams before any grating diffraction. Next, we introduce diffraction due to a grating and explore the impact on the phase terms.

2.3. Effects from astigmatism upon diffraction

The effect of diffraction into various angles which are different from the angle of incidence can be accounted for by introducing an *astigmatism* to the Gaussian beam. As demonstrated in Fig. 1 (left), a beam incident on the grating will possess different angles of incidence and reflection, i.e. $\alpha \neq \beta$. Consequently, the diffracted beam produces an elliptical beam spot, only the beam parameters along the x-axis change, whilst those along the y-axis remain the same. This astigmatism results in a different waist size along the x-axis in the diffracted beam, $\omega_{0_r}^x$, which can be expressed in terms of the waist size of the incident beam, ω_{0_i}, using the following relation

$$\omega_{0_r}^x = \omega_{0_i}\frac{\cos\beta}{\cos\alpha}. \tag{7}$$

Note that for the incident beam, the waist size ω_{0_i} is identical in both x and y-directions, and for the diffracted beam, the waist size in the y-direction remains unchanged, implying that $\omega_{0_r}^y = \omega_{0_i}$. From Eq. (1), we let $d = 1666\,\text{nm}$ and $\alpha = 10^\circ$ to give $\beta_1 = 27.7^\circ$. If $\omega_{0_i} = 10\,\text{mm}$, then according to Eq. (7), $\omega_{0_r}^x = 8.99\,\text{mm}$. Using these specific values and Eqs. (14) and (15), the phase of each beam after being diffracted by the grating (and at a distance z away from the waist position) was plotted against x (the radial distance from the central optical axis), creating the phase distributions seen in Fig. 2. Compared to the non-displaced beam

#187849 - $15.00 USD Received 27 Mar 2013; revised 11 Oct 2013; accepted 16 Oct 2013; published 22 Nov 2013

(blue solid line), the phase distribution of a geometrically translated beam (green solid line) displays the same shape and profile, and is shifted by an amount h along the x-axis, clearly noticeable in Fig. 2. The phase for a modally decomposed beam (red solid line) exhibits the same distribution profile, also shifted by h, yet an additional shift along the y-axis is evident, giving rise to 'negative' phase. This effect can be clarified by Eq. (15) in Appendix B: the nature of the equation constricts the phase distribution for the modally decomposed beam such that the phase equals zero when $x = 0$ and $x = 2h$, and hence the reason for the overlap of the red and blue traces at $x = 0$ where there is zero phase.

Subsequently, we find that increasing values of h leads to further phase deviation of the modally decomposed beam from the geometrically translated beam. This is simply due to a violation in the approximation $h/\omega_0 \ll 1$, which was used to obtain Eq. (5) and in turn Eq. (15).

For comparison, the phase distributions for the non-displaced, geometrically translated and modally decomposed beams before grating diffraction are also included (dashed lines). Notice that although the phase of the non-diffracted beams present a wider distribution, deviating away from the solid lines when further away from the optical axis (as one would expect), the general profile of the dashed traces is similar to the solid traces and displays no phase difference at the central optical axis of the beams.

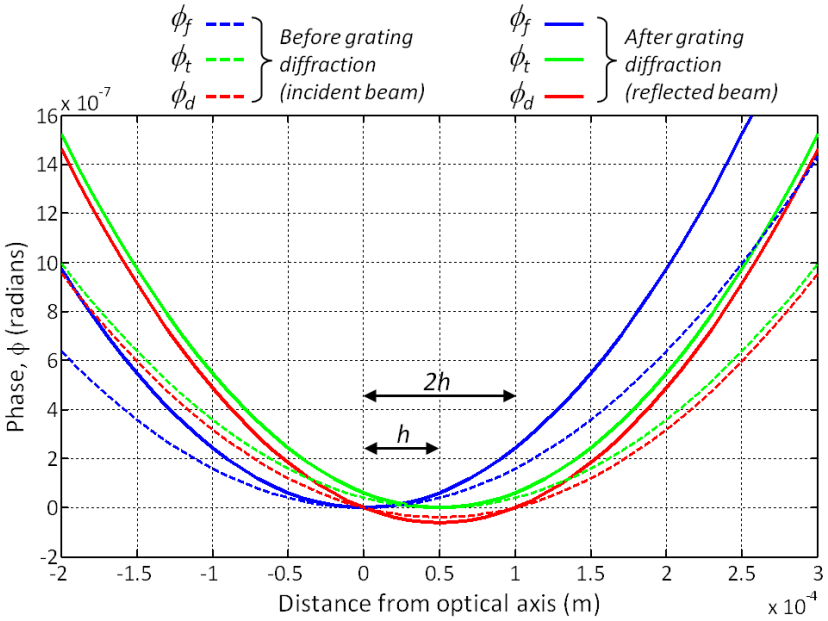

Fig. 2. Beam phase (wave front) for a fundamental non-translated beam (solid blue), translated beam (solid green) and a modally decomposed beam (solid red). For comparison, the dashed lines represent the corresponding beams before grating diffraction. The following parameters are assumed: $h = 0.05$ mm, $\lambda = 10^{-6}$ m, $z = 0.5$ m, $\omega_{0_i} = 10$ mm and $\omega_{0_r}^x = 8.99$ mm.

2.4. *Analytical results*

Although the beam suffers from astigmatism as a result of grating diffraction, this does not change the overall wave front for a geometrically translated or modally decomposed beam, relative to a non-displaced beam. Within the Gaussian framework (using Eq. (6)), we find that when a beam is displaced (either through a geometrical translation or modal decomposition)

#187849 - $15.00 USD Received 27 Mar 2013; revised 11 Oct 2013; accepted 16 Oct 2013; published 22 Nov 2013

in increments of increasing h, the phase distribution is always the same. For example, for a geometrically translated beam, the phase at the central optical axis is always zero, regardless of the value of h. We can therefore verify that our Gaussian-based framework does not include a change in phase of 2π in the order of the grating period (i.e. $\Delta x' = d$) [11], contrary to the requirements given in Eq. (2). The absence of the expected phase change is due to the fact that the geometrical layout in our framework of beam displacement is not interchangeable with that of a grating displacement.

It should be noted that the use of only one higher-order mode to describe the beam shift introduces small phase differences and a full expansion into more modes would mitigate this. However, in this discussion we are aiming at identifying phase terms in the order of 1 radian and thus the simple approximation of using only the first higher-order mode is sufficient.

We now aim to test the validity of the modal decomposition technique when describing diffracted displaced beams: we analyse the phase between various orders of beam modes through experimental means and justify whether adding the higher-order mode to the fundamental mode is acceptable.

3. An experimental demonstration of phase and mode independency

The modal expansion is using the fact that different fields in a linear optical system can be computed separately and then superimposed to calculate the total field. In order to further validate this method in the context of diffraction gratings we use a table-top experiment to establish that after grating diffraction, the phase of a zero-order (TEM_{00}) beam and a first-order (TEM_{10}) beam are the same, thus signifying that the phase of a diffracted beam is independent of its mode and thus independent of the intensity pattern.

3.1. Experimental setup

A grating Mach-Zehnder interferometer was developed and used to distinguish the phase between zero-order and first-order modes, as depicted in Fig. 3. The laser beam was guided through a series of modematching lenses and steering mirrors before entering the triangular mode-cleaner (MC). The MC was tuned by means of a piezoelectric transducer (PZT), the position of which altered the round-trip distance of the circulating light inside the MC, and thereby allowing any chosen mode to resonate and pass through. The beam was split into two arms of equal lengths via an input beamsplitter (BS). A ruled reflective diffraction grating was located in one arm, with a grating period of $d = 1666.7$ nm and aligned to reflect in the first diffraction order. Note that for the purpose of this experiment, the grating was fixed in position and was not translated in any direction. The other arm contained a second PZT, providing a slight modulation to the arm-length. Both beams recombined and interfered at the output BS, creating a pair of output beams. Each output beam consisted of two superimposed beams: grating arm in transmission plus PZT arm in reflection (denoted as the 'east port' in Fig. 3), and grating arm in reflection plus PZT arm in transmission (designated as the 'south port').

3.2. Dual-mode locking system

The MC operates using feedback control based on the Pound-Drever-Hall scheme [15]. The zero-order and first-order modes resonating within the MC were isolated and enhanced using a combination of steering mirrors. The distance between the resonant peaks of the two modes determined the amplitude of a square-wave signal (which in this case was 2.1 V), which in turn was injected into the MC. The square-wave signal caused the PZT to jump back and forth between two very specific positions, coinciding with the zero-order and first-order mode resonances, as revealed by the green trace in Fig. 4 (set at a frequency of 3 Hz). As a result, a stable

#187849 - $15.00 USD Received 27 Mar 2013; revised 11 Oct 2013; accepted 16 Oct 2013; published 22 Nov 2013

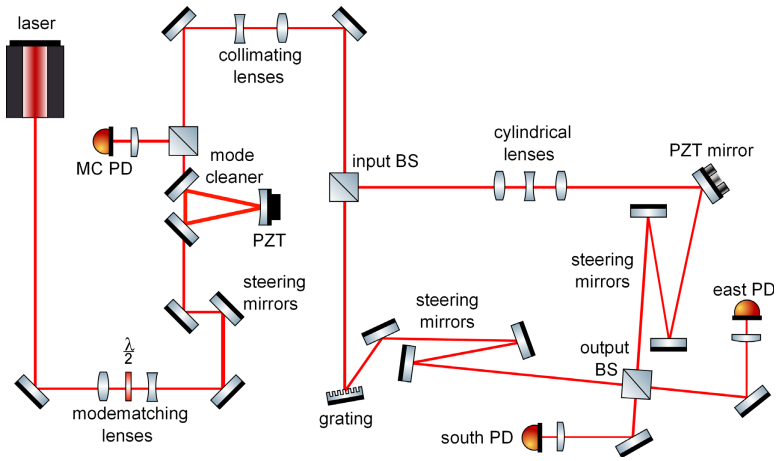

Fig. 3. Layout of a grating Mach-Zehnder interferometer. A square-wave signal is injected into the mode-cleaner, allowing the instrument to lock to zero-order and first-order mode resonances alternately. One arm of the interferometer accommodates the diffraction grating, whilst the length of the other arm is subjected to tiny fluctuations to create interfering fringe signals at the output.

lock to the two alternating modes was successfully achieved, signified by the emission of a high and constant level of light power from the MC (blue trace in Fig. 4).

In response to the PZT modulation in the Mach-Zehnder arm (purple trace in Fig. 4), the superimposed output beams undergo constructive and destructive interference periodically, and photodetectors (PDs) situated at each output port detect a fringe pattern of light and dark bands. Note that when the east port PD senses constructive interference, the south port PD observes destructive interference, and vice versa. The red trace in Fig. 4 is the resulting wave formed from the interference fringes as detected by the south port PD.

A number of breaks within the fringe waveform are clearly noticeable in Fig. 4, corresponding with the vertical dashed lines. We identified that these disruptions coincide precisely with the moment when the square-wave signal jumps between the modes. Small additional distortions can also be seen at these times, and are caused by the temporary disruption of the servo control due to the jump. The breaks in fringe symmetry are due to the change in direction by the PZT mirror in the Mach-Zehnder arm, hence the correlation with the peaks and troughs of the triangular wave, indicated by the vertical dotted lines in Fig. 4.

3.3. Experimental results

If the phase in the zero-order and first-order modes were different, one would expect a noticeable shift in the phase of the fringe signal when the modes switched, i.e., at the instant when the square-wave ramp stepped either up or down. Instead, the results in Fig. 4 (red trace) show a continuous and unbroken fringe signal during mode-switching, with no obvious deviation from the general waveform. The absence of a shift in phase in the fringe signal confirms the absence of a significant phase difference between both the zero-order and first-order modes after grating diffraction. This supports the assumption that the phase of a diffracted beam is independent of the beam shape.

#187849 - $15.00 USD Received 27 Mar 2013; revised 11 Oct 2013; accepted 16 Oct 2013; published 22 Nov 2013

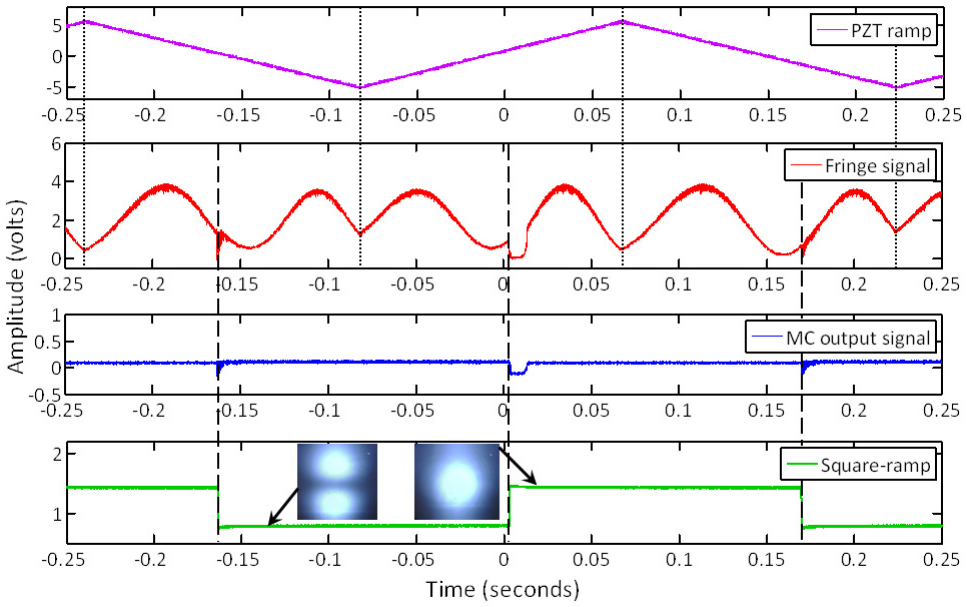

Fig. 4. Interference fringe signal during mode-switching. From top to bottom: PZT modulation signal in one of the Mach-Zehnder arms (purple); fringe signal due to interference at the east port (red); output signal from the MC (blue); square-wave signal applied to the MC to ramp between modes (green), where the maximum and minimum part of the signal correspond to the zero-order and first-order mode resonances respectively. As the system switches between the modes, the waveform of the fringe signal continues undisturbed - this effect is only achieved when the phase of each mode is the same. Note that the slight fluctuations visible in the fringe signal (and simultaneously in the output of the MC) are due to the stabilisation effects of the electronics when locking to each mode.

4. A rigorous simulation tool for beam diffraction

Through the use of simulation techniques, we verify with greater certainty whether or not the phase of a diffracted beam is independent of its shape, and we subsequently aim to compare the phase profile of a diffracted beam when applying the modal decomposition method with the phase profile of an actual beam displacement. The simulation relies on a comprehensive technique known as a Finite-Difference Time-Domain (FDTD) analysis, which can be utilised to create a powerful two-dimensional simulation tool to solve Maxwell's equations rigorously in the time-domain [16, 17]. For our purposes, an FDTD implementation was developed [18] to investigate how beam/grating displacements coupled into the phase of diffraction orders. A key element is that the FDTD analysis allows for the simulation of Gaussian beams, which is not the case for other significant approaches, such as the Rigorous Coupled-Wave Analysis (RCWA), based on the planewave approximation. The FDTD analysis enabled us to simulate a diffraction grating and propagate beams with orders of various mode, and thereby study the phase changes created when the beam or grating is displaced. The main objective is to understand why the periodic change in phase of 2π radians (a definitive outcome for a displaced beam in a geometric sense) is absent from the analytical model for a modally decomposed beam in Section 2.

#187849 - $15.00 USD Received 27 Mar 2013; revised 11 Oct 2013; accepted 16 Oct 2013; published 22 Nov 2013

4.1. *Main parameters and optical layout*

The properties of the modelled optical layout and diffraction grating are shown in Table 1. The cell size, Δ, determines the resolution of the simulation space - a smaller cell size results in a higher resolution. For our purpose, the simulation considers only the $m = 0$ and $m = \pm 1$ diffraction orders, and the diffraction angle is set at $\pm 45^\circ$ so as to minimise anisotropic dispersion.

Table 1. Parameter values used to simulate Gaussian beam diffraction by a grating.

Parameter name	Parameter value
Cell size, Δ	25 nm
Simulation dimension	$1300\Delta \times 1800\Delta = 32.5\,\mu$m $\times$ 45 μm
Wavelength, λ	1064 nm
Grating period, d	60Δ = 1500 nm
Beam propagation distance, z	1200Δ = 30 μm
Radius of beam waist, ω_0	100Δ = 2500 nm

The concept of the simulation is as follows: a Gaussian beam is propagated through a diffraction grating to create $m = 0$ and $m = \pm 1$ diffraction orders. For simplicity, a transmission grating is used instead of a reflection grating - this avoids the need to model a reflective coating, while the results regarding the phase changes remain the same.

Figure 5 presents an instantaneous image of a diffraction pattern for a TEM_{00} beam (left), and a TEM_{10} beam (right). The beam travels in the direction indicated by the red arrow, and the stationary grating is shown by the dashed grey lines.

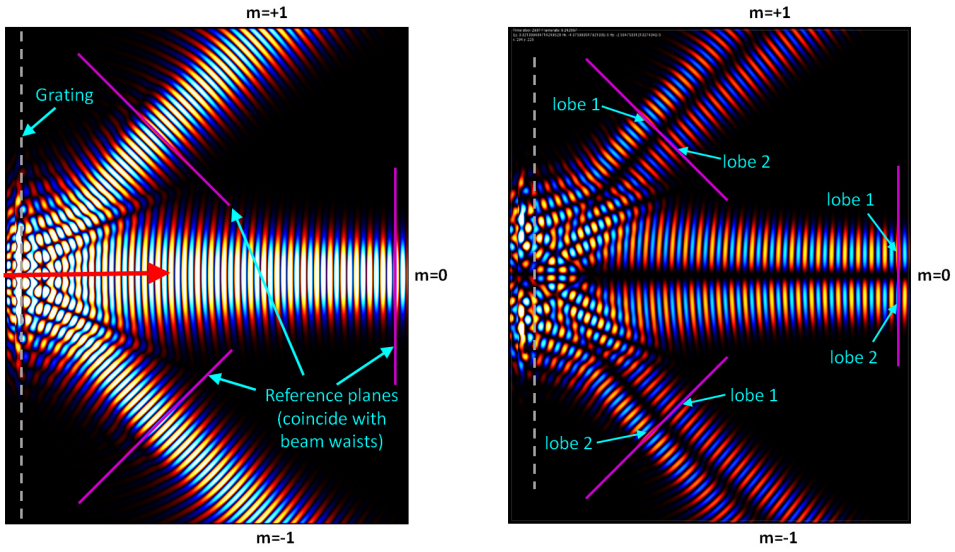

Fig. 5. Diffraction patterns formed by a TEM_{00} beam (left) and a TEM_{10} (right). The beams propagate through the diffraction grating (dashed grey lines), and the phase for each diffraction order, $m = 0$ and $m = \pm 1$, is measured at the reference planes (solid pink lines).

After diffraction, each beam continues to propagate until they encounter reference planes,

#187849 - $15.00 USD Received 27 Mar 2013; revised 11 Oct 2013; accepted 16 Oct 2013; published 22 Nov 2013

visible as straight, solid pink lines in Fig. 5. Along each reference plane, a probe sits at the point of maximum intensity and measures the phase of the passing beam. Since a TEM_{10} beam consists of two intensity spots (or lobes), each reference plane contains two probes for phase measurement, as indicated in Fig. 5 (right). We positioned the reference planes to coincide with the beam waist in all diffraction orders so as to avoid any extra Gouy phase effects in beams of higher order modes. For measurements involving grating displacements, the distance of the grating period d was divided into 40 steps, and the grating was translated incrementally by a distance of $d/40$ each time. The total displacement of the incident beam (or grating) was therefore equivalent to a distance of one grating period ($1.5\,\mu$m), i.e., $\Delta x' = d$. At each grating position, the probes recorded the phase and the simulation was run for some time to allow for better averaging. The simulation was executed in order to explore two different scenarios:

1. Displacing the incident beam (or grating) vertically using a TEM_{00} beam. Note that the context of beam displacement and grating displacement are interchangeable if the geometrical layout is the same. However, when the beam is displaced in the simulation, the reference planes do not follow suit and remain static (see Fig. 5). For this reason, it is necessary to also translate the reference planes vertically, simultaneously with beam displacement, ensuring that the geometry of the layout with respect to the grating is consistent.

2. Modal decomposition, adding a TEM_{10} beam gradually to a TEM_{00} beam (thereby reproducing a vertical beam displacement, in accordance with Eq. (5)). This scenario introduces two possibilities: (a) moving the reference planes simultaneously in a vertical direction, for reasons of consistency as described in the first scenario, and (b) without moving the reference planes. The latter raises an interesting issue: given the fact that simulations based on modal decomposition are unable to automatically change coordinate systems, it follows that the reference planes (along which the phase is measured) also remain static during beam displacement. We therefore wish to investigate both possibilities (a) and (b).

4.2. Simulation results

The change in phase for the three separate cases outlined above in 1, 2(a) and 2(b) are presented in Fig. 6. Each diffraction order is indicated by the following trace colours: green ($m = 0$), red ($m = +1$) and blue ($m = -1$). The various line styles represent each scenario: beam/grating displacement (solid), modally decomposed with vertical movement of reference planes (dotted) and modally decomposed without movement of reference planes (dashed).

4.2.1. Beam/grating displacement

During displacement of the grating (or beam) using a TEM_{00} mode beam, the phase remains constant for $m = 0$ (solid green). For $m = +1$ (solid red), the phase gradually increases, and for $m = -1$ (solid blue), the phase decreases. In each case, the phase undergoes a linear change of 2π radians over a total displacement of d. The opposite sign of the slopes are accounted for by the direction of the grating or beam translation; the optical path length increases in one of the first diffraction orders and decreases in the other. The profile of these traces are as predicted by Eq. (2).

4.2.2. Modal decomposition - reference planes translated vertically

When a TEM_{10} mode is added to a TEM_{00} mode beam, the result is a TEM_{00} beam displaced along the vertical axis (parallel to the grating). As a higher portion of TEM_{10} is added, the resulting beam experiences a further displacement. Repositioning the reference planes along the

#187849 - $15.00 USD Received 27 Mar 2013; revised 11 Oct 2013; accepted 16 Oct 2013; published 22 Nov 2013

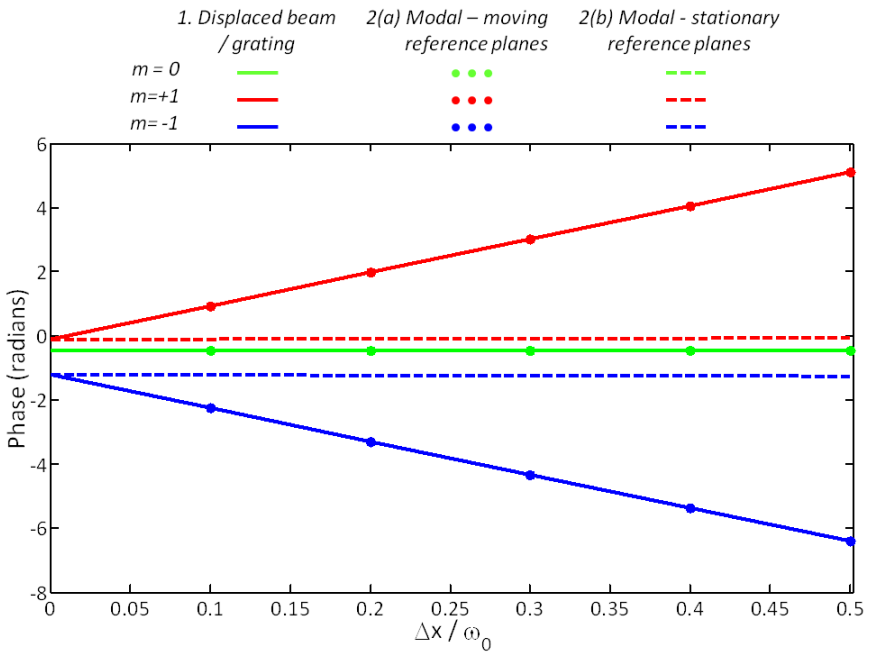

Fig. 6. Phase changes for a displaced beam after grating diffraction, as measured in the $m = 0$ and $m = \pm 1$ diffractive orders. Three cases are considered: beam/grating displacement (solid), modal decomposition with reference planes adjusted vertically (dotted), and modal decomposition with fixed reference planes (dashed). Note that the green dashed line is coincident with the green solid line.

vertical axis simultaneously with the resulting beam displacement ensures a consistent geometric layout with respect to the grating.

During the addition of the higher-order mode, the phase is seen to be unchanging for $m = 0$ (dotted green), and the phase in the $m = +1$ (dotted red) and $m = -1$ (dotted blue) either increase or decrease, respectively. The phase profiles exhibited in this scenario are highly comparable with the profiles from the first scenario, and we can confidently conclude that the addition of a first-order mode to a zero-order mode beam is an accurate description for small beam or grating displacements in terms of the phase changes produced.

4.2.3. Modal decomposition - stationary reference planes

A TEM_{10} mode beam was added to a TEM_{00} mode beam and produced a TEM_{00} beam displaced along the vertical axis, as described before. However, since the reference planes remained static, after each addition of the higher-order mode (equivalent to each step of a beam or grating translation), the total optical path length between the grating and the reference plane increased in one of the first diffractive orders and decreased in the other (depending on the direction of the resulting beam displacement). In fact, fixing the reference planes in one position exactly compensates for the previously seen linear phase profile, hence we obtain flat lines for $m = 0$ (dashed green, which is not visible because it exactly coincides with the solid green trace), $m = +1$ (dashed red) and $m = -1$ (dashed blue).

It is important to note that optical simulation tools used to study alignment issues, such as FINESSE, are restricted in that computations can only be carried out in one coordinate system. It is for this reason that these simulation tools rely on the modal decomposition method for

#187849 - $15.00 USD Received 27 Mar 2013; revised 11 Oct 2013; accepted 16 Oct 2013; published 22 Nov 2013

replicating beam displacements. However, the single coordinate system also means that the reference planes are also forced to remain stationary, as described in the scenario 2(b). We have shown here that in this situation the phase change due to beam translation on a diffraction grating is not contained in the usual model and we recommend a manual injection of this phase into the analytical model and into existing Gaussian-based simulation tools in order to obtain an accurate description of the beam when interacting with diffractive elements.

5. Conclusion

It has been proposed to use diffraction gratings in high-precision laser interferometers such as modern gravitational wave detectors. However, further research has identified an additional, possibly critical, alignment induced phase noise related to diffraction gratings. In this paper we report our investigation towards a mathematical framework which allows implementing this noise effect in commonly used analytical and numerical models for laser interferometers. We have successfully developed a framework for describing the phase effects due to beam translations on diffractive elements, incorporating a Gaussian model. We analysed the modal model for a diffracted Gaussian beam and determined that the usual modal model does not account for the phase change for translated or misaligned beams. Using an experimental setup we demonstrated the absence of phase changes between a diffracted zero-order beam and first-order beam. Consequently, we confirmed that the phase of a diffracted Gaussian beam is completely independent of the beam shape, and that the inclusion of higher-order modes has no effect on the overall phase. Using a dedicated simulation tool, we examined the phase changes in the first diffraction order for two scenarios: firstly during beam/grating displacement for a zero-order beam and secondly by modal decomposition. We confirmed that the phase changes resulting from grating displacement were in agreement with a pure geometric planewave consideration. It is essential that the reference planes, and therefore the coordinate system, can be moved in order to obtain the correct phase measurements when reproducing beam displacements. In a fixed coordinate system required for the common application of modal models, this can accounted for most easily by adding the extra phase change relating to the change in the geometric path length when a beam is displaced. This is valid for analytical and numerical models, and we suggest implementing this procedure to Gaussian-based simulations relying on modal decomposition, such as FINESSE.

Appendix A: Mathematical derivation of a Gaussian beam

We present a mathematical description of Gaussian beams in more detail here. Hermite-Gauss modes have the general form:

$$E(x,y,z) = \sum_{nm} a_{nm}(x,y,z)u_{nm}(x,y,z)e^{-ikz}. \tag{8}$$

The normalised Hermite-Gauss function $u_{nm}(x,y,z)$ describes the transverse spatial distribution of the beam as it varies slowly with z and is defined as:

$$\begin{aligned} u_{nm}(x,y,z) &= \left(2^{n+m-1}n!m!\pi\right)^{\frac{1}{2}} \frac{1}{\omega(z)} \exp\big(i(n+m+1)\Psi(z)\big) H_n\left(\frac{\sqrt{2}x}{\omega(z)}\right) \\ &\times H_m\left(\frac{\sqrt{2}y}{\omega(z)}\right) \exp\left(-i\frac{k(x^2+y^2)}{2R_C(z)} - \frac{x^2+y^2}{\omega^2(z)}\right), \end{aligned} \tag{9}$$

where H_n and H_m are Hermite polynomials, $\omega(z)$ is the beam size, $R_C(z)$ is the radius of curvature of the beam wavefronts. The Gouy phase is specified as $\Psi(z) = \arctan[(z-z_0)/z_R]$, with

#187849 - $15.00 USD Received 27 Mar 2013; revised 11 Oct 2013; accepted 16 Oct 2013; published 22 Nov 2013

z_R being the Rayleigh range. Unless otherwise specified, the beam waist, ω_0, will always be located at the grating, i.e. where $z = z_0$.

In general, an offset beam is displaced in both the x and y directions. Due to the symmetry of the system, we consider the displacement of the beam for only one degree of freedom, along the x-axis. The normalised Hermite-Gauss function, $u_n(x,z)$ in x becomes:

$$u_n(x,z) = \left(\frac{2}{\pi}\right)^{\frac{1}{4}} \left(\frac{\exp\big(i(2n+1)\Psi(z)\big)}{2^n n!\,\omega(z)}\right)^{\frac{1}{2}} H_n\left(\frac{\sqrt{2}x}{\omega(z)}\right) \exp\left(-i\frac{kx^2}{2R_C(z)} - \frac{x^2}{\omega^2(z)}\right). \quad (10)$$

At the waist, the Gouy phase is zero. In addition, $R_C \to \infty$ and therefore the R_C term in Eq. (10) can be ignored. Since $H_0 = 1$, a zero-order mode where $n = 0$ can be described at the waist position in the following form:

$$u_0(x,z_0) = \left(\frac{2}{\pi}\right)^{\frac{1}{4}} \frac{1}{\sqrt{\omega_0}} \exp\left(-\frac{x^2}{\omega_0^2}\right). \quad (11)$$

A first-order mode with $n = 1$ at the waist position is given as:

$$u_1(x,z_0) = \left(\frac{2}{\pi}\right)^{\frac{1}{4}} \frac{1}{\sqrt{2\omega_0}} \left(\frac{2\sqrt{2}x}{\omega_0}\right) \exp\left(-\frac{x^2}{\omega_0^2}\right). \quad (12)$$

Using Eqs. (11) and (12), we obtain a simple relationship between the zero-order and first-order modes at the beam waist:

$$u_1(x,z_0) = \frac{2x}{\omega_0} u_0(x,z_0). \quad (13)$$

Appendix B: Derivation of phase terms

In Section 2.2, the phase, θ, is described for a stationary fundamental beam (f), a translated beam (t) and a modally decomposed beam (d). The common factor of $kz - \frac{1}{2}\Psi$ in Eq. (6) can be omitted to leave $\phi_{f,t,d}$, defined for each individual beam as follows:

$$\phi_f = \frac{kx^2}{2R_C}, \qquad \phi_t = \frac{k(x-h)^2}{2R_C}, \qquad \phi_d = \frac{kx^2}{2R_C} - \varphi. \quad (14)$$

The φ term in Eq. (14) arises from the fact that the beam in Eq. (5) is a superposition of modes. By expanding and simplifying Eq. (5), we find that the remaining factor consists of a sum of terms, which is subsequently treated as a complex number. We use the relation $e^{i\varphi} = (\cos\varphi + i\sin\varphi)$ to reach the expression:

$$\varphi = \arctan\left(\frac{\sin\Psi}{\cos\Psi + \left(\frac{\omega\,\omega_0}{2xh}\right)}\right). \quad (15)$$

Acknowledgment

This work was funded by the Science and Technology Facilities Council (STFC).

#187849 - $15.00 USD Received 27 Mar 2013; revised 11 Oct 2013; accepted 16 Oct 2013; published 22 Nov 2013